

Figure 1. Five WGM Resonators are arranged to form a filter chain. Through adjustment of gaps and voltages, guided by monitoring of optical power levels, desired transfer function ( $P_{out}/P_{in}$  versus frequency detuning) can be obtained. The underlying principles of design and operation are also applicable to a chain of more or fewer than five WGM resonators.

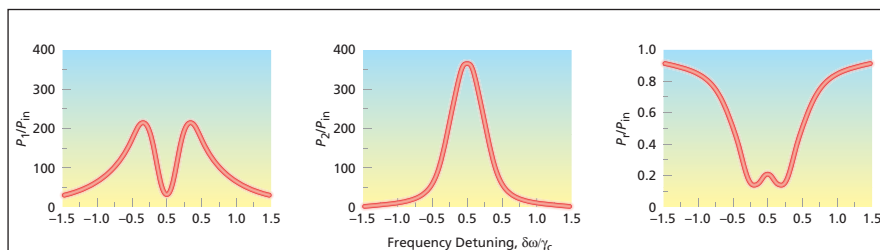


Figure 2. These Curves Represent Optimal Coupling of the first two resonators in an intermediate step toward realizing a fifth-order Butterworth filter. On the abscissa,  $\delta\omega$  denotes the frequency detuning and  $\gamma_c$  denotes the full frequency width of the resonance spectral peak at half maximum in the fully loaded condition.

and still others monitor the input power ( $P_{in}$ ) and output power ( $P_o$ ). The readings of these photodiodes are used to guide the tuning adjustments described below.

The steps of the first procedure are the following:

1. Uncouple all the resonators and prisms by increasing all the gaps.
2. Overload resonator 1 with the input coupling prism, then measure the input power ( $P_{in}$ ), reflected power ( $P_r$ ), and the power in resonator 1 ( $P_1$ ) as functions of frequency detuning from resonance, and use the measure-

ment data to determine the resonance quality factor ( $Q$ ).

3. Couple resonator 2 to resonator 1, then measure  $P_{in}$ ,  $P_r$ ,  $P_1$ , and  $P_2$  as functions of frequency detuning from resonance. Adjust the gap between resonators 1 and 2 until  $P_r/P_{in}$ ,  $P_1/P_{in}$ , and  $P_2/P_{in}$  as functions of frequency detuning match a set of theoretical template functions (see Figure 2) calculated to contribute to the desired high-order transfer function.
4. Couple resonator 3 to resonator 2, then measure  $P_{in}$ ,  $P_r$ ,  $P_1$ ,  $P_2$ , and  $P_3$  as functions of frequency detuning from reso-

nance. Adjust the gap between resonators 2 and 3 until  $P_r/P_{in}$ ,  $P_1/P_{in}$ , and  $P_2/P_{in}$  as functions of frequency detuning match a different set of theoretical template functions calculated to contribute to the desired high-order transfer function.

5. Repeat step 4, each time adding the next resonator (and then adding the output coupling prism after the last resonator has been added) and adjusting the gaps to obtain the desired responses.

The steps of the second procedure are the following:

1. Measure and tabulate the dependence of each resonance frequency of each resonator on the bias voltage applied to that resonator.
2. Introduce, into the filter operation, "dark" periods, during which the laser and the resonators are scanned over some finite frequency band.
3. During a dark period, apply a specified voltage to resonator 1 to shift its resonance frequency by some amount. Measure the shift, then compensate it by applying another voltage to shift the resonance to the middle of the scan of the laser frequency.
4. Repeat step 3 for resonator 2 and subsequent resonators except the last one.
5. Adjust the voltage on the last resonator to scan its frequency until the filter exhibits maximum transmission, at which point the desired high-order transfer function has been restored.

*This work was done by Andrey Matsko, Anatoliy Savchenkov, Dmitry Strelakov, and Lute Maleki of Caltech for NASA's Jet Propulsion Laboratory. Further information is contained in a TSP (see page 1).*

*The software used in this innovation is available for commercial licensing. Please contact Karina Edmonds of the California Institute of Technology at (626) 395-2322. Refer to NPO-43872.*

## Robust Mapping of Incoherent Fiber-Optic Bundles

Images scrambled by the bundles can be unscrambled.

Marshall Space Flight Center, Alabama

A method and apparatus for mapping between the positions of fibers at opposite ends of incoherent fiber-optic bundles have been invented to enable the use of such bundles to transmit images in visible or infrared light. The method is robust in the sense that it provides useful mapping even for a bundle that contains thousands

of narrow, irregularly packed fibers, some of which may be defective.

In a coherent fiber-optic bundle, the input and output ends of each fiber lie at identical positions in the input and output planes; therefore, the bundle can be used to transmit images without further modification. Unfortunately, the

fabrication of coherent fiber-optic bundles is too labor-intensive and expensive for many applications. An incoherent fiber-optic bundle can be fabricated more easily and at lower cost, but it produces a scrambled image because the position of the end of each fiber in the input plane is generally different from

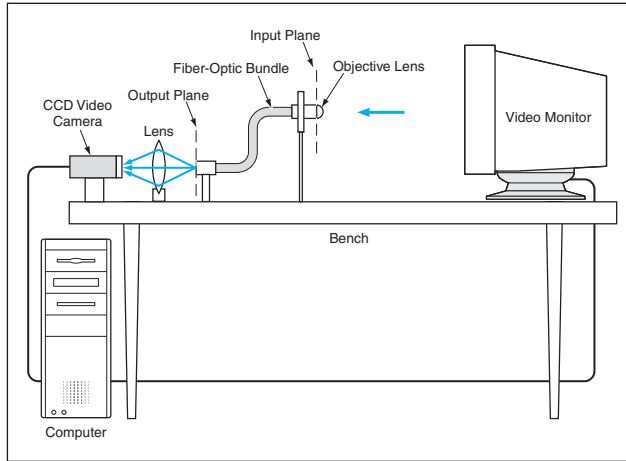


Figure 1. Test Patterns Are Generated on the video monitor and imaged onto the input end of the fiber-optic bundle. The resulting scrambled images that appear on the output end of the bundle are analyzed to determine a mapping between the input and output fiber ends.

the end of the same fiber in the output plane. However, the image transmitted by an incoherent fiber-optic bundle can be unscrambled (or, from a different perspective, decoded) by digital processing of the output image if the mapping between the input and output fiber-end positions is known. Thus, the present invention enables the use of relatively inexpensive fiber-optic bundles to transmit images.

The invention calls for a two-part calibration or mapping process. Part 1 of the process (ordinarily performed by the fiber-bundle supplier) takes place on the apparatus depicted in Figure 1. A computer that controls the apparatus and processes its measurement causes a video monitor to generate a test pattern described below. The input end of the fiber-optic bundle is equipped with an objective lens and is positioned so that the test pattern on the video monitor is focused onto the input plane. Another lens focuses the image from the output plane onto a charge-coupled-device (CCD) video camera. The output of the camera is digitized and fed to a frame grabber in the computer.

At first, the test pattern is a solid bright screen, so that the output ends of all the fibers (except the defective ones) appear bright. The digitized image of the output plane is subjected to a sequence of digital processing steps in which the centroids of the output-fiber-end subimages are computed, as illustrated in the upper part of Figure 2. Thereafter, these centroids are deemed to be the positions of the output fiber ends for the purpose of mapping.

As shown in the lower part of Figure 2, a test pattern in the form of a bright horizontal line is then swept vertically across the input end, in increments correspon-

ding to one pixel of the CCD; at each increment of position, the brightness at each pixel location on the CCD is recorded. Next, the same thing is done with a test pattern in the form of a bright vertical line swept horizontally. On the basis of the brightness-vs.-pixel-position data from the horizontal and vertical sweeps, the horizontal and vertical line positions that result in maximum brightnesses at the

previously determined centroids are computed. These horizontal and vertical line positions are converted to coordinates of fiber ends on the input plane. Thus, the relationship between the coordinates of the input and output ends of each and every fiber (not including defective fibers) is established. This relationship, which is the desired mapping, is recorded in a lookup table (LUT). Each fiber-optic bundle is characterized by a unique LUT.

The mapping as determined thus far is unique to the pixel coordinate system and the setup of the mapping apparatus; as such, the mapping is subject to change along with changes in magnification, translation, and rotation of images when the fiber bundle is removed from the mapping apparatus and installed in another apparatus in which it

is to be used to transmit images. The mapping as determined thus far is also subject to change associated with focus adjustments, change of the CCD camera, or insertion or removal of an infrared or visible-light filter in the image-transmission system.

Part 2 of the calibration process involves a partial remapping to compensate for such changes. Part 2 (ordinarily performed by the end user) takes place once the fiber-optic bundle has been installed in the imaging system. The input end of the bundle is illuminated with a solid bright test pattern and the user visually compares the video image of the output end with the corresponding image recorded previously in the first step of Part 1. The user identifies the ends of four fibers in the two images for use as fiducial points. Then software computes a preliminary new LUT based on the previous LUT and the coordinates of the fiducial points in the previous and present coordinate systems. The new LUT can be tested visually by computing the output fiber centroids and overlaying them on the video image. If necessary, the transformation coefficients can be modified in an iterative subprocess until the fiber centroids computed by use of the new LUT appear to lie at the centers of the fibers in the video image.

*This work was done by Harry E. Roberts, Brent E. Deason, Charles P. DePlachett, Robert A. Pilgrim, and Harold S. Sanford of SRS Technologies for Marshall Space Flight Center. Further information is contained in a TSP (see page 1). MFS-31520*

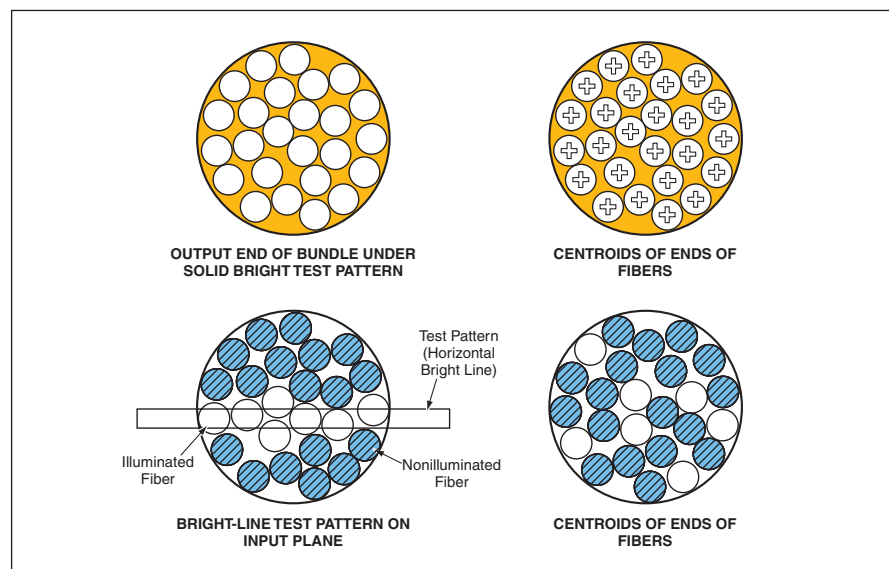


Figure 2. Centroids of Output Fiber Ends are computed in the first step of part 1 of the calibration procedure. The relationship between coordinates of input and output ends is determined from image data acquired in sweeps of horizontal and vertical bright lines across the input plane.